

Intention Learning From Human Demonstration*

HOA-YU CHAN, KUU-YOUNG YOUNG⁺ AND HSIN-CHIA FU

Department of Computer Science

⁺*Department of Electrical Engineering*

^{*}*Vision Research Center*

National Chiao Tung University

Hsinchu, 300 Taiwan

Equipped with better sensing and learning capabilities, robots nowadays are meant to perform versatile tasks. To remove the load of detailed analysis and programming from the engineer, a concept has been proposed that the robot may learn how to execute the task from human demonstration by itself. Following the idea, in this paper, we propose an approach for the robot to learn the intention of the demonstrator from the resultant trajectory during task execution. The proposed approach identifies the portions of the trajectory that correspond to delicate and skillful maneuvering. Those portions, referred to as motion features, may implicate the intention of the demonstrator. As the trajectory may result from so many possible intentions, it poses a severe challenge on finding the correct ones. We first formulate the problem into a realizable mathematical form and then employ the method of dynamic programming for the search. Experiments based on the pouring and also fruit jam tasks are performed to demonstrate the proposed approach, in which the derived intention is used to execute the same task under different experimental settings.

Keywords: intention learning, human demonstration, motion feature, robot imitation, skill transfer

1. INTRODUCTION

Robot applications nowadays are extended from the organized factories to the uncertain home environments, thanks to the progress of the sensing and learning techniques. Meanwhile, as the robot may face many complicated tasks in daily life, it will then demand much effort from the human operator for detailed task analysis and program coding. To avoid this, researchers have proposed letting the robot learn how to execute the task from observing human demonstration by itself [1]. Among them, Asfour, *et al.* proposed integrating multiple human demonstrations for robot motion generation using Hidden Markov models [2]. Dautenhahn and Nehaniv proposed an approach for the robot to learn from human demonstration by imitation, referred to as the correspondence problem [3], and later the team developed the JABBERWOCKY system for 2D arranging tasks [4, 5]. Aleotti, *et al.* [6, 7] and also Ekvall and Kragic [8] proposed methods for the robot to learn the pick-and-place task from human demonstrations. And, Ogawara, *et al.* proposed a hybrid frame-work which combines the reusable symbol task and precise skill in trajectory level for general 3D object-operating tasks [9, 10]. In these researches, one issue of focus is how to cut the motions correctly to match with the corresponding human intentions. Some

Received July 23, 2009; revised January 20 & March 12, 2010; accepted March 24, 2010.

Communicated by Pau-Choo Chung.

* Part of this paper has been presented at National Symposium on System Science and Engineering, Taiwan, 2008. This work was supported in part by the National Science Council of Taiwan, R.O.C., under grant No. NSC 96-2628-E-009-164-MY3, and also Department of Industrial Technology under grant No. 97-EC-17-A-02-S1-032.

proposed cutting the motions at the points of low speeds [11, 12]. However, the human operator may then have to slow down the motion intentionally during demonstration. As an alternative, Chalodhorn, *et al.* proposed a motion cutting method corresponding to cyclic motions, which demands the operator to perform certain type of motions [13]. Baldwin and Baird claimed that babies of 7-8 month old can cut motions by regular pattern, while it is still unclear of the cutting process [14]. Calinon, *et al.* [15] presented a programming by demonstration framework for generically extracting the relevant feature of a given task and for addressing the problem of generalizing the acquired knowledge to different contexts.

In this paper, we also propose an approach for the robot to learn the human intention from her/his demonstration. The proposed approach does not constrain the human operator to perform the task with certain motion speed or motion type, and also allows the order of the events to be altered during demonstration. The approach identifies the portions of the trajectory corresponding to the delicate and dexterous maneuver of the demonstrator, referred to as motion features. These motion features, in some sense, exhibit the human skill in executing a certain task. The challenge for the proposed approach is how to find those correct intentions, among all possible ones, that lead to the demonstrated trajectories. To tackle the complexity in search, we first formulate the problem into the mathematical form and then apply the method of dynamic programming for the search [16]. Experiments based on the pouring task are performed to demonstrate the proposed approach first. During the experiments, the locations of the vessels and the pouring sequence may vary, and the motion features derived from the demonstrated trajectories are used to execute the pouring task under different experimental settings. To further explore its generality, we also apply the proposed approach for a fruit jam task, in which the robot learns how to spread fruit jam on toast.

2. PROPOSED APPROACH

Many daily works involve the interactions between tools and objects [9]. The resultant trajectory during the working process can be basically divided into two types of motions: delicate motion (D) for delicate maneuver and move motion (M) between the delicate motions [10]. The delicate motion is more of the focus, since it serves to achieve the goal of the work; by contrast, the move motion is not that critical. Therefore, in this paper, we take the intention finding problem to be that of locating the delicate motion from the demonstrated trajectory. Fig. 1 shows the conceptual diagram of the proposed approach for intention learning from human demonstration. In Fig. 1, the robot first observes a series of human demonstrations and records the corresponding trajectories and environmental states. From these recorded motion data, the robot searches for the possible intentions that lead to the delicate motions. The derived intentions can then be used to generate new trajectories

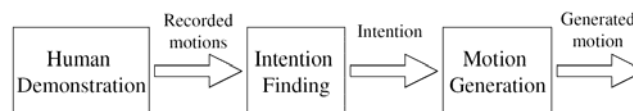


Fig. 1. The conceptual diagram of the proposed approach for intention learning from human demonstration.



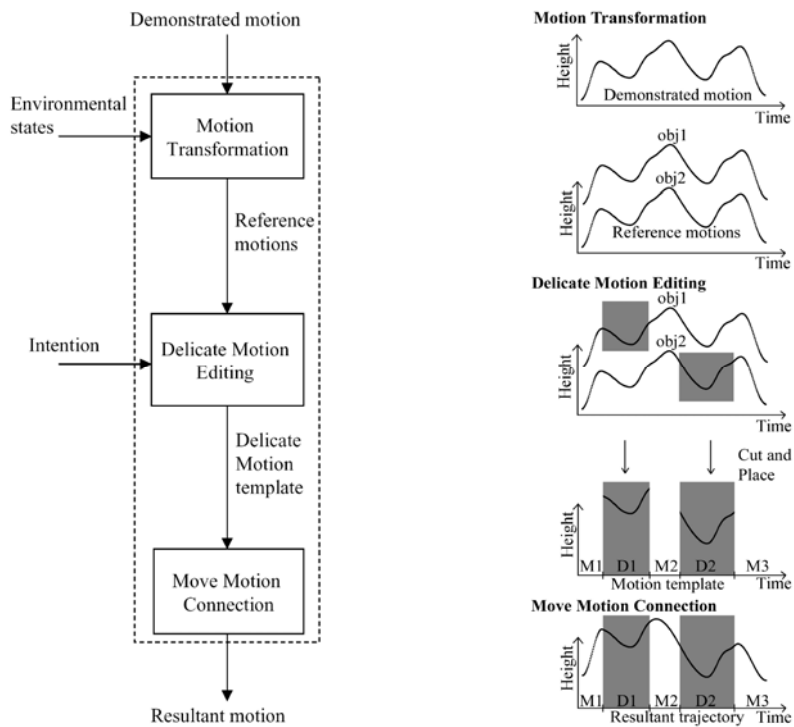
(a) The setting of the vessels. (b) Pouring vessel A to vessel B. (c) Pouring vessel A to vessel C.

Fig. 2. A pouring task with its motion sequence.

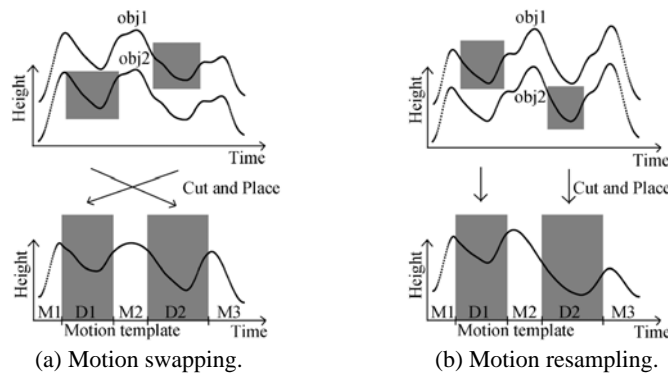
responding to new environmental states. Take the pouring task shown in Fig. 2 as an example. In Fig. 2 (a), three vessels A, B, and C are arbitrarily located on the table. In Figs. 2 (b) and (c), the operator pours the content from vessel A to vessels B and C, respectively, and then places vessel A back on the table. During the demonstrations, the initial locations of the vessels may vary, and so does the pouring sequence. From the recorded trajectories and corresponding initial locations of the vessels (environmental states), the proposed approach will identify the intention of the operator, *i.e.*, the portions of the trajectory that correspond to the pouring action. With the derived intention, the robot is now ready to execute the pouring task with the vessels located at various locations and possibly altered pouring sequences.

Fig. 3 (a) shows the proposed motion generation process under new environmental states, and Fig. 3 (b) an illustrative example based on the pouring task shown in Fig. 2. In Fig. 3 (a), the inputs are the environmental states and the demonstrated motion for which the optimal intention is derived. The demonstrated motion serves to provide the delicate motions associated with the intention. However, this demonstrated motion cannot be used for reference directly, for being facing different environmental states. As illustrated in Fig. 3 (b), in responding to the new initial locations of vessels B and C, two reference motions are generated according to the demonstrated motion. It is because we do not know which object each of the delicate motions is associated with in advance, we thus generate these two reference motions by assuming all the delicate motions are associated with either *Obj1* or *Obj2* alone. Meanwhile, the height of *Obj1* being higher than that of *Obj2* is just for simplicity in illustration. *Obj1* can be higher, equal to, or lower than *Obj2*, depending on its actual location. In the next step, the intention is sent into the delicate motion editing module, which will then cut out the delicate motions from those reference motions accordingly. Fig. 3 (b) shows that the input intention identifies the parts of the motions containing the lower heights (marked by the grey box) as the delicate motions (indicating the pouring action). Up to now, we have a motion template filled with several isolated delicate motions, as shown in Fig. 3 (b). The move motions are then used to connect these delicate motions. As its accuracy is not that critical, the move motion is generated using the cubic polynomial. Finally, a feasible trajectory corresponding to the new environmental state is generated.

One point that deserves discussions for this trajectory generation process is about the delicate motion editing. Because the operator may perform the demonstrations in different speeds and possibly with different orders for the events involved, the corresponding delicate motions are likely to be with various sampling rates, or to appear in different portions of the demonstrated trajectories. Therefore, the delicate motion editing may not always be as straightforward as that shown in Fig. 3 (b). Fig. 4 shows another two possible cases for



(a) The process. (b) An illustrative example based on the pouring task.
 Fig. 3. Motion generation from the derived intention under new environmental states.



(a) Motion swapping. (b) Motion resampling.
 Fig. 4. Two cases for delicate motion editing.

delicate motion editing. Fig. 4 (a) shows the situation that the two delicate motions swap their mapping during motion editing, corresponding to the alternation of the event order. Fig. 4 (b) shows that for the resampling of the delicate motions, corresponding to the different motion speeds during task execution. Consequently, it can be expected that there will be many possible matches present between the intention and the corresponding delicate motions, which highly complicates the following intention finding process.

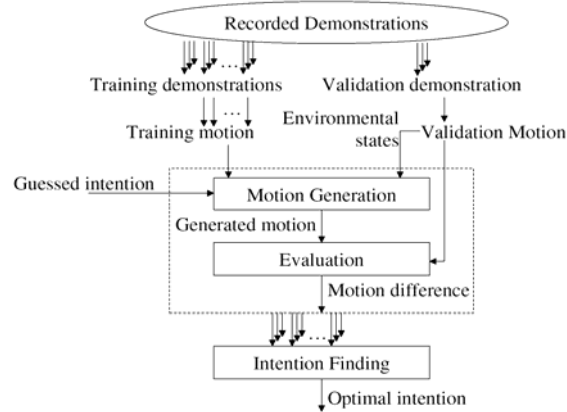


Fig. 5. The process of intention finding from the recorded demonstrations.

2.1 Intention Finding

Fig. 5 shows the process of intention finding from the recorded demonstrations. It is assumed that each of the demonstrated trajectories includes all the delicate motions, but some of them are allowed to be with extra or redundant motions. And, the duration of the delicate and move motions is set to be longer than 0.3 second, as human cannot cognize an event until it happens 0.3 second later [17]. In Fig. 5, among all the recorded demonstrations, one demonstration is first selected as the validation demonstration, and the rest as the training demonstrations, for each sequence of the process. The process will be repeated until each of the recorded demonstrations serves as the validation demonstration once. The reasoning behind the design in Fig. 5 is that the optimal intention derived from the training demonstrations should lead to a generated motion that best matches a validation demonstration involving only necessary delicate motions. During the process, the dotted block in Fig. 5 is used for the comparison between the validation motion and the generated motion from the motion generation module, discussed in the previous section. The inputs to this motion generation module are the training motion and the environmental states corresponding to the validation motion, along with a guessed intention, acting as a possible intention for the validation motion. Because the proposed approach does not constrain the human operator to perform the task with certain motion speed or motion type, and also allows the order of the events to be altered during demonstration, there is in fact no prior knowledge for the selection of the guessed intention. Therefore, we take every portion of the trajectory of the validation demonstration as the candidate for the guessed intention, if only its duration is longer than 0.3 second. Consequently, there will be a huge number of possible intentions to serve as the guessed intentions for each of the training-validation demonstration pairs. The method of dynamic programming is thus employed for the search. Finally, judging from all those motion differences, the intention finding module determines the optimal intention for the recorded demonstrations.

For mathematical formulation of this intention finding process [16], we start with the representation of the intention I . Assume that there are N delicate motions and S objects involved in a demonstrated task. Because the intention is closely related to the deli-

cate parts of the maneuver, I is formulated as a set of delicate motions, $D_n(t)$, associated with the corresponding objects Obj_s :

$$I = \{D_1(t), D_2(t), \dots, D_N(t); Obj_1, Obj_2, \dots, Obj_s\} \quad (1)$$

where $D_n(t)$ stands for the part of the demonstrated trajectory for delicate motion n and Obj_s the position and orientation of an object s . Note that, because an object may correspond to one, several, or no delicate motion, the number of delicate motions may not be equal to that of the objects. Following the process shown in Fig. 5, I_V , as a guessed intention for a given validation motion $Q_V(t)$, is sent into the motion generation module, along with the training motion $Q_T(t)$ and the environmental states Obj_s for $Q_V(t)$. A given delicate motion $D_{V_i}(t)$ for I_V can then be formulated as

$$D_{V_i}(t) = \{\{Q_V(n_i), Q_V(n_i + 1), \dots, Q_V(n_i + L_{n_i})\}, s_i\} \quad (2)$$

where $D_{V_i}(t)$ stands for the part of the demonstrated trajectory for a delicate motion i , $Q_V(t)$ the point on $D_{V_i}(t)$ with n_i and L_{n_i} the starting time and time length for $D_{V_i}(t)$, respectively, and s_i the index linking $D_{V_i}(t)$ to the object s . For each Obj_s , the motion generation module, shown in Fig. 3 (a), first generates reference motions based on $Q_T(t)$. According to I_V , the module will then cut out the corresponding delicate motions $D_G(t)$ from these reference motions. Finally, move motions $M_G(t)$ are employed for smooth connection between every two adjacent $D_G(t)$, and $D_G(t)$ and $M_G(t)$ together form the trajectory $Q_G(t)$ for I_V . As its demand on accuracy is not strict, $M_G(t)$ is formulated as the cubic polynomial, described by

$$M_G(t) = at^3 + bt^2 + ct + d \quad (3)$$

where parameters $a \sim d$ can be determined by the four constraints resulting from the requirement that the positions and velocities of the points connecting $M_G(t)$ with the two adjacent $D_G(t)$ must be continuous.

To determine the optimal intention I_V^* for the selected validation motion, $Q_V(t)$ will be compared with all $Q_G(t)$ generated according to every guessed intention I_V . Because we are looking for an intention that may induce all the necessary delicate motions, I_V^* should not cause too much deviation between $Q_V(t)$ and every $Q_G(t)$ generated for each training motion. By taking E_{\max} as the maximum difference between $Q_V(t)$ and those Q_G generated for all the training motions corresponding to some intention I_V , we determine I_V^* , among all I_V , to be the one that leads to the smallest E_{\max} , and formulate the criterion as

$$I_V^* = \arg \min_{I_V} E_{\max} \quad (4)$$

with

$$E_{\max} = \max_i \|Q_V(t) - Q_G^i(t)\|^2 \quad (5)$$

where the function argmin yields the value of the given argument for which the value of the given expression attains its minimum value and i is the index for the training motions.

Because each recorded demonstration will serve as the validation demonstration once, the optimal intention I_V^{**} for the demonstrator will be further chosen as that I_V^* , among those for each validation motion, with the smallest corresponding E_{\max} , denoted as E^* . To note that, E^* for each I_V^* needs to be normalized before the comparison, since the length L_V for each validation motion may not be the same. I_V^{**} is then formulated as

$$I_V^{**} = \arg \min_{I_V^*} E^* / L_V. \quad (6)$$

The key to the success of this intention finding process is to efficiently find I_V^* described in Eq. (4). However, the search involved in Eq. (4) is of high complexity. Let us evaluate the comparison between $Q_V(t)$ and $Q_G(t)$ first. As mentioned before, the operator may execute the demonstrations with different speeds or event orders. Consequently, for an intention I_V guessed for $Q_V(t)$, the search for finding its corresponding delicate motions from those reference motions for $Q_T(t)$ will face way too many alternatives. To reduce the search complexity, we performed the comparisons only for those involving similar $D_V(t)$ and $D_G(t)$ (an approach analogous to that of dynamic time warping [18]), which would lead to small differences. To further reduce the complexity, we also propose dividing the comparison of $Q_V(t)$ and $Q_G(t)$ into those of their delicate motions, $D_V(t)$ and $D_G(t)$, and move motions, $M_V(t)$ and $M_G(t)$, respectively, and revise Eq. (4) to be

$$I_V^* = \arg \min_{I_V} \left(\sum_{j=1}^N \max_i \|D_{V_j}(t) - D_{G_j}^i(t)\|^2 + \sum_{j=1}^{N+1} \max_i \|M_{V_j}(t) - M_{G_j}^i(t)\|^2 \right). \quad (7)$$

In Eq. (7), the matches between I_V and its corresponding delicate motions are, in a sense, executed within several smaller search spaces. As a further attempt to enhance search efficiency, we go on to reformulate Eq. (7) into Eq. (8), described by

$$I_V^* = \arg \min_{I_V} \left(\left(\sum_{j=1}^k \max_i \|D_{V_j}(t) - D_{G_j}^i(t)\|^2 + \sum_{j=1}^k \max_i \|M_{V_j}(t) - M_{G_j}^i(t)\|^2 \right) + \left(\sum_{j=k+1}^N \max_i \|D_{V_j}(t) - D_{G_j}^i(t)\|^2 + \sum_{j=k+1}^{N+1} \max_i \|M_{V_j}(t) - M_{G_j}^i(t)\|^2 \right) \right). \quad (8)$$

The formulation in Eq. (8) exhibits an appealing feature very suitable for realization via dynamic programming, for being able to be tackled through an expansion into several sub-searching ones recursively [16]. In Eq. (8), its first part is intended to find the E_{\max} for j from 1 to k , and the second part that for j from $k+1$ to N (plus that for the last move motion). A recursive formulation for computing E^* can then be established by assuming k to be an N , starting from $k=1$, described as

$$E^* = \min_{D_N \in \text{all } D} (E_R(D_N) + E_M(D_N, D_{N+1})) \quad (9)$$

with

$$E_R(D_k) = \min_{D_{k-1}} (E_R(D_{k-1}) + E_M(D_{k-1}, D_k)) + E_D(D_k) \quad (10)$$

where E_R stands for the minimum difference between the motions from the first move mo-

tion to a given (assumed to be N) delicate motion (in Eq. (9), it is D_N ; in Eq. (10), it is D_k or D_{k-1}), E_M the difference for the move motion between two delicate motions, and E_D the difference for a given delicate motion. Note that, the first move motion is generated between D_0 and D_1 , and the last one between D_N and D_{N+1} , with D_0 and D_{N+1} taken as the first and last point of the trajectory, respectively. In Eq. (9), E^* is derived as the minimum for all $E_R(D_N)$ with $E_R(D_N)$ computed recursively from Eq. (10). With Eqs. (9) and (10), dynamic programming can take advantage of those tables generated for $E_R(D_k)$ to simplify the computation in deriving I_V^* .

Finally, the time complexity for the process of dynamic programming, which is related to the number (R) and length (L_V) of the demonstrations and the number (S) of objects involved in the task, is computed to be in the order of $O(R \cdot L_V^5 \cdot S^2)$, discussed below. From Eqs. (9) and (10), the time complexity results mainly from generating the tables for $E_R(D_k)$, which involves L_V and S . The table for $E_R(D_k)$ has $O(L_V^2 \cdot S)$ elements, and each element deals with $E_M(D_{k-1}, D_k)$ and $E_R(D_{k-1})$ for $O(L_V^2 \cdot S)$ times. The time complexity for computing $E_M(D_{k-1}, D_k)$, which involves R and L_V , is $O(R \cdot L_V)$, while $E_R(D_{k-1})$ can be found from the tables directly. Therefore, the total time complexity is computed to be approximately $O(R \cdot L_V^5 \cdot S^2)$. Note that, the number of delicate motions (N) is not shown in $O(R \cdot L_V^5 \cdot S^2)$, because the proposed approach takes every portion of the trajectory of the validation demonstration as the candidate for a possible delicate motion, its effect has been incorporated into the formula already.

Based on the discussions above, the algorithm for intention finding is formulated as follows,

Algorithm for intention finding: Find the intention of the demonstrator through R times of demonstrations.

- Step 1:** Record the demonstrated trajectories for the R times of demonstrations. Denote the recorded trajectory for the i th demonstration as $Q_i(t)$. Set $i = 1$.
- Step 2:** Select $Q_i(t)$ among the R recorded trajectories as the validation motion Q_V and the rest as the training motions $Q_T(t)$.
- Step 3:** Apply the method of dynamic programming, based on Eqs. (9) and (10), to determine the optimal intention I_V^* for $Q_V(t)$. Let $i = i + 1$. If $i \leq R$, go to step 2; otherwise, go to step 4.
- Step 4:** Utilize Eq. (6) to determine the optimal intention I_V^{**} for the demonstrator among those for the R validation motions. I_V^{**} is now ready to be used for executing the task under new environmental states.

3. EXPERIMENT

To validate its feasibility, we applied the proposed approach for the pouring task shown in Fig. 2 first. The experiment was divided into two stages: (a) human demonstration and (b) robot execution. Fig. 6 (a) shows the experimental setup for human demonstration, which includes the human operator and the electromagnetic motion tracking system (FASTRAK, manufactured by Polhemus, USA). In Fig. 6 (a), the human operator held a vessel (vessel A) and poured the content into the two vessels (vessels B and C) on the table in an arbitrary order. A total of ten demonstrations of the pouring task had been

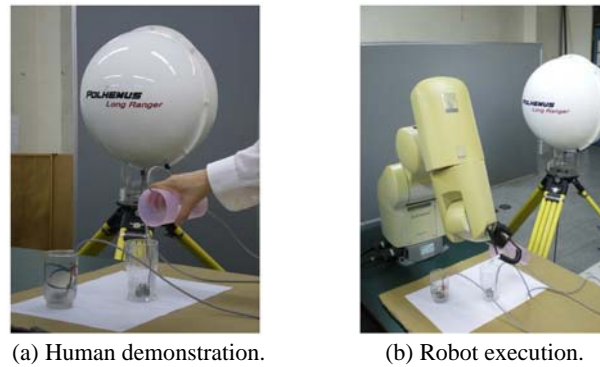


Fig. 6. Experimental setups for the pouring task.

performed, with the locations of vessels A, B, and C varied during each demonstration. The Polhemus FASTRAK tracking system, with a sampling rate of 40 Hz for each of the sensors, was used to measure and record the demonstrated trajectories and positions of the objects. These trajectories were recorded as the 7-dimensional sequences, which consist of positions and orientations (in the form of quaternion) in 3 and 4 dimensions, respectively, with the position normalized by its standard deviation. From these recorded trajectories, we applied the intention finding algorithm, discussed in section 2.1, to derive the intention of the operator from all possible intentions, with a total number approximating 10^{22} . During intention derivation, we combined two adjacent delicate motions when they were related to the same vessel and also executed in the same order for all the ten demonstrated trajectories, so as to avoid too many small delicate motions. We then moved on to the second stage of the experiment, and let the Mitsubishi RV-2A 6-DOF robot manipulator follow the derived intention to execute the pouring task under new environmental states, as shown in Fig. 6 (b).

Fig. 7 shows the derived intentions for each of the ten demonstrations of the pouring task. In Fig. 7, delicate motions related to vessels B and C were identified from the trajectory of vessel A, marked by the blue and green blocks, respectively. It was observed that most of the delicate motions were located at those portions with minimum heights, implicating the pouring action. The derived intention for demonstration 5 was determined to be optimal among all. We then let the robot manipulator follow this intention to execute the pouring task, in which vessels B and C were placed in new locations. For comparison, the human operator was also asked to execute the same pouring task. Fig. 8 (a) shows the variations of the height of vessel A during task execution, Fig. 8 (b) its trajectories in the X-Y plane, and Fig. 8 (c) the variations of its tilt angle. These three trajectories for the human operator and robot manipulator exhibited certain degree of similarity, but not exactly the same. Meanwhile, the robot manipulator successfully accomplished the pouring task.

To further explore its generality, we also apply the proposed approach for a fruit jam task, in which the robot learns how to spread fruit jam on toast. Fig. 9 shows the experimental setup, which was also divided into the stages of (a) human demonstration and (b) robot execution. In Fig. 9 (a), the human operator picked up a knife from the table, scooped the fruit jam from the jar, spread it on the toast in a zigzag motion, and then placed the

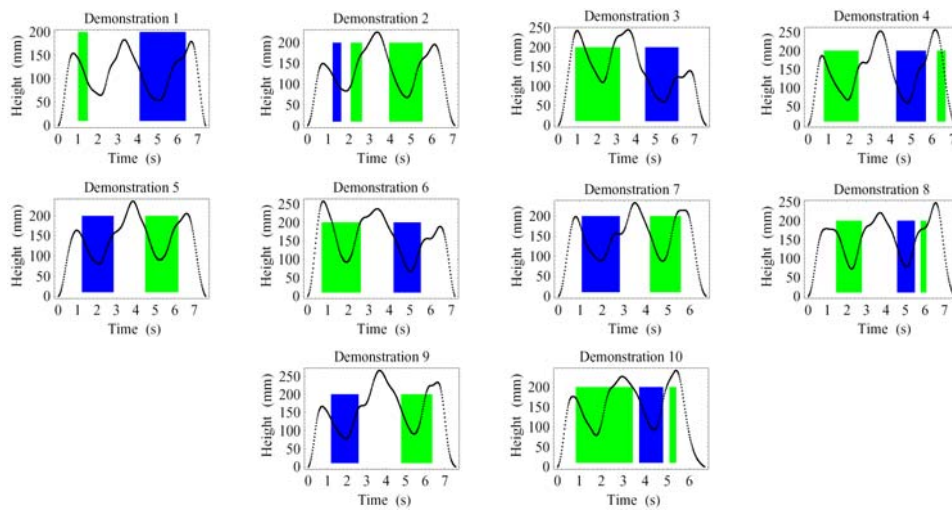
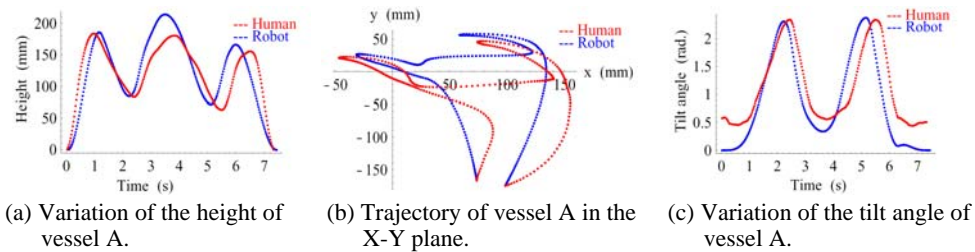


Fig. 7. The derived intentions for the ten demonstrations of the pouring task.

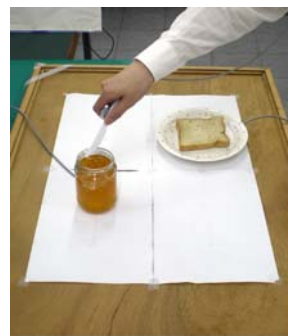


(a) Variation of the height of vessel A.

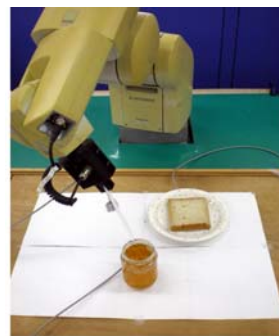
(b) Trajectory of vessel A in the X-Y plane.

(c) Variation of the tilt angle of vessel A.

Fig. 8. Experimental results for the pouring task executed by both the human operator and robot manipulator under new environmental states.



(a) Human demonstration.



(b) Robot execution.

Fig. 9. Experimental setups for the fruit jam task.

knife back on the table. A total of ten demonstrations had been performed, with the locations of the knife, jar, and toast varied during each demonstration. The intention finding algorithm was then applied to derive the intention of the operator from all possible intentions, with a total number approximating 10^8 .

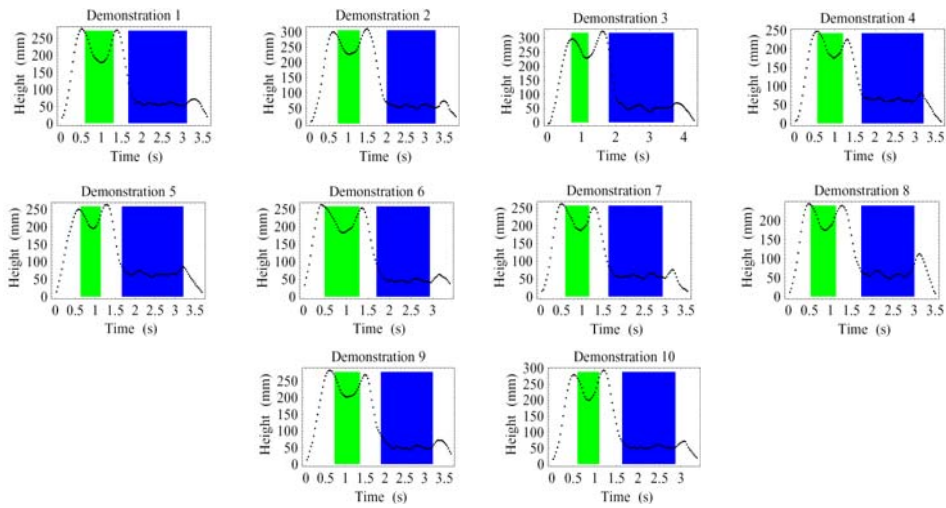


Fig. 10. The derived intentions for the ten demonstrations of the fruit jam task.

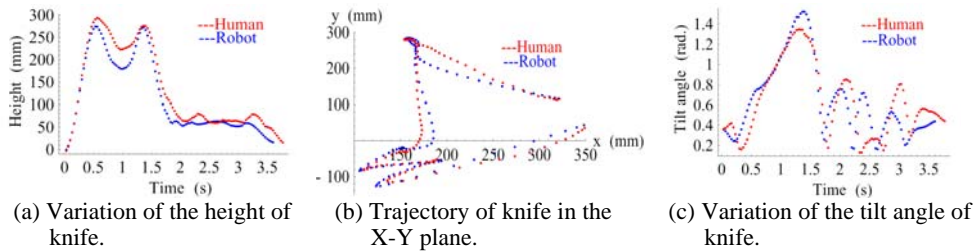


Fig. 11. Experimental results for the fruit jam task executed by both the human operator and robot manipulator under new environmental states.

Fig. 10 shows the derived intentions for each of the ten demonstrations. In Fig. 10, delicate motions related to the jar and toast were identified from the trajectory of the knife, marked by the green and blue blocks, respectively. It was observed that these two delicate motions were located at the portions of the first local minimum and a following flat region, implicating the scooping and zigzag motions. The derived intention for demonstration 1 was determined to be optimal. We then let the robot manipulator utilize this intention to execute the fruit jam task, in which the jar and toast were placed in new locations. And, the human operator was also asked to execute the same task. Fig. 11 (a) shows the variations of the height of the knife during task execution, Fig. 11 (b) its trajectories in the X-Y plane, and Fig. 11 (c) the variations of its tilt angle. Similar to the phenomenon exhibited in the pouring task, the trajectories for the human operator and robot manipulator were not exactly the same, while the robot manipulator successfully accomplished the task.

4. CONCLUSION

In this paper, we have proposed an approach for the robot to derive the intention of

the human operator from her/his demonstration. The proposed approach does not demand the operator to slow down the motion speed or follow a pre-specified order or motion pattern during task execution, so that the demonstration can be executed in a natural manner. For system implementation, we have first formulated this intention finding problem into a realizable mathematical form, and then applied the method of dynamic programming for the search. Experiments based on the pouring and also fruit jam tasks have validated its feasibility. Although only three objects and two operations were involved in the tasks for demonstration, the proposed approach is not limited by the number of objects or operations. In future works, we will further investigate its scalability and generality. We will also apply the proposed approach to derive intentions for more versatile and complicated tasks.

REFERENCES

1. Y. Kuniyoshi, M. Inaba, and H. Inoue, "Learning by watching: Extracting reusable task knowledge from visual observation of human performance," *IEEE Transactions on Robotics and Automation*, Vol. 10, 1994, pp. 799-822.
2. T. Asfour, F. Gyarfas, P. Azad, and R. Dillmann, "Imitation learning of dual-arm manipulation tasks in humanoid robots," in *Proceedings of IEEE-RAS International Conference on Humanoid Robots*, 2006, pp. 40-47.
3. K. Dautenhahn and C. L. Nehaniv, "The correspondence problem," *Imitation in Animals and Artifacts*, 2002, pp. 41-61.
4. A. Alissandrakis, C. L. Nehaniv, K. Dautenhahn, and J. Saunders, "Using JABBER-WOCKY to achieve corresponding effects: Imitating in context across multiple platforms," in *Proceedings of International Workshop on the Social Mechanisms of Robot Programming by Demonstration*, 2005, pp. 9-12.
5. A. Alissandrakis, C. L. Nehaniv, K. Dautenhahn, and J. Saunders, "Achieving corresponding effects on multiple robotic platforms: Imitating in context using different effect metrics," in *Proceedings of the 3rd International Symposium on Imitation in Animals and Artifacts*, 2005, pp. 10-19.
6. J. Aleotti, S. Caselli, and M. Reggiani, "Toward programming of assembly tasks by demonstration in virtual environments," in *Proceedings of IEEE International Workshop on Robot and Human Interactive Communication*, 2003, pp. 309-314.
7. J. Aleotti, S. Caselli, and M. Reggiani, "Leveraging on a virtual environment for robot programming by demonstration," *Robotics and Autonomous Systems*, Vol. 47, 2004, pp. 153-161.
8. S. Ekvall and D. Kragic, "Integrating object and grasp recognition for dynamic scene interpretation," in *Proceedings of IEEE International Conference on Advanced Robotics*, 2005, pp. 331-336.
9. K. Ogawara, J. Takamatsu, H. Kimura, and K. Ikeuchi, "Extraction of fine motion through multiple observations of human demonstration by DP matching and combined template matching," in *Proceedings of IEEE International Workshop on Robot and Human Interactive Communication*, 2001, pp. 8-13.
10. K. Ogawara, J. Takamatsu, H. Kimura, and K. Ikeuchi, "Extraction of essential interactions through multiple observations of human demonstrations," *IEEE Transactions*

- on Industrial Electronics*, Vol. 50, 2003, pp. 667-675.
11. O. C. Jenkins and M. J. Mataric, "Deriving action and behavior primitives from human motion data," in *Proceedings of IEEE Conference on Intelligent Robots and Systems*, 2002, pp. 2551-2556.
 12. M. J. Mataric, "Sensory-motor primitives as a basis for imitation: Linking perception to action and biology to robotics," *Imitation in Animals and Artifacts*, 2002, pp. 391-422.
 13. R. Chalodhorn, K. MacDorman, and M. Asada, "Automatic extraction of abstract actions from humanoid motion data," in *Proceedings of IEEE/RSJ International Conference on Intelligent Robots and Systems*, 2004, pp. 2781-2786.
 14. D. A. Baldwin and J. A. Baird, "Discerning intentions in dynamic human action," *Trends in Cognitive Sciences*, Vol. 5, 2001, pp. 171-178.
 15. S. Calinon, F. Guenter, and A. Billard, "On learning, representing and generalizing a task in a humanoid robot," *IEEE Transactions on Systems, Man and Cybernetics, Part B*, Vol. 37, 2007, pp. 286-298.
 16. T. H. Cormen, C. E. Leiserson, and R. L. Rivest, *Introduction to Algorithms*, MIT Press, Cambridge, Massachusetts, 1990.
 17. S. Sutton, M. Braren, J. Zublin, and E. John, "Evoked potential correlates of stimulus uncertainty," *Science*, Vol. 150, 1965, pp. 1187-1188.
 18. H. Sakoe and C. Chiba, "Dynamic programming algorithm optimization for spoken word recognition," *IEEE Transactions on Acoustics, Speech, and Signal Processing*, Vol. 26, 1978, pp. 43-49.



Hoa-Yu Chan (陳豪宇) received the B.S. degree from National Central University in Computer Science and Information Engineering in 2000, and the M.S. degree in 2002 from National Chiao Tung University in Computer Science and Information Engineering, where he is currently working toward the Ph.D. degree. His research interests include machine learning, imitation learning, and robot programming by demonstration.



Kuu-Young Young (楊谷洋) was born in Kaohsiung, Taiwan, 1961. He received his B.S. degree in Electrical Engineering from National Taiwan University, Taiwan, in 1983, and M.S. and Ph.D. degrees in Electrical Engineering from Northwestern University, Evanston, IL, U.S.A., in 1987 and 1990, respectively. Between 1983 and 1985, he served as an electronic officer in Taiwan Navy. Since 1990, he has been with the Department of Electrical Engineering at National Chiao Tung University (NCTU), Hsinchu, Taiwan, where he is currently a Professor. He served as the chairman of the department from 2003 to 2006, and the associate dean

of Electrical and Computer Engineering College, NCTU, from 2007 to 2010. His research interests include robot compliance control, robot learning control, robot calibration and path planning, teleoperation, brain computer interface, and Science, Technology, and Society (STS).



Hsin-Chia Fu (傅心家) received the B.S. degree from National Chiao Tung University in Electrical and Communication Engineering in 1972, and the M.S. and Ph.D. degrees from New Mexico State University, both in Electrical and Computer Engineering in 1975 and 1981, respectively. From 1981 to 1983, he was a Member of the Technical Staff at Bell Laboratories. Since 1983, he has been on the faculty of the Department of Computer Science and Information Engineering at National Chiao Tung University, in Taiwan, R.O.C. He is also the Taiwan representative of TEI Consortium since 2003. His research interests include digital signal/image processing, multimedia information processing, web image search, and neural networks. He has been the Technical Committee on Neural Networks for Signal Processing of the IEEE Signal Processing Society from 1997 to 2000. He has authored more than 100 technical papers, and two textbooks “PC/XT BIOS Analysis,” and “Introduction to Neural Networks,” by Sun-Kung Book Co., and Third Wave Publishing Co., respectively. Dr. Fu is a member of the IEEE Signal Processing and Computer Societies, Phi Tau Phi, and the Eta Kappa Nu Electrical Engineering Honor Society.